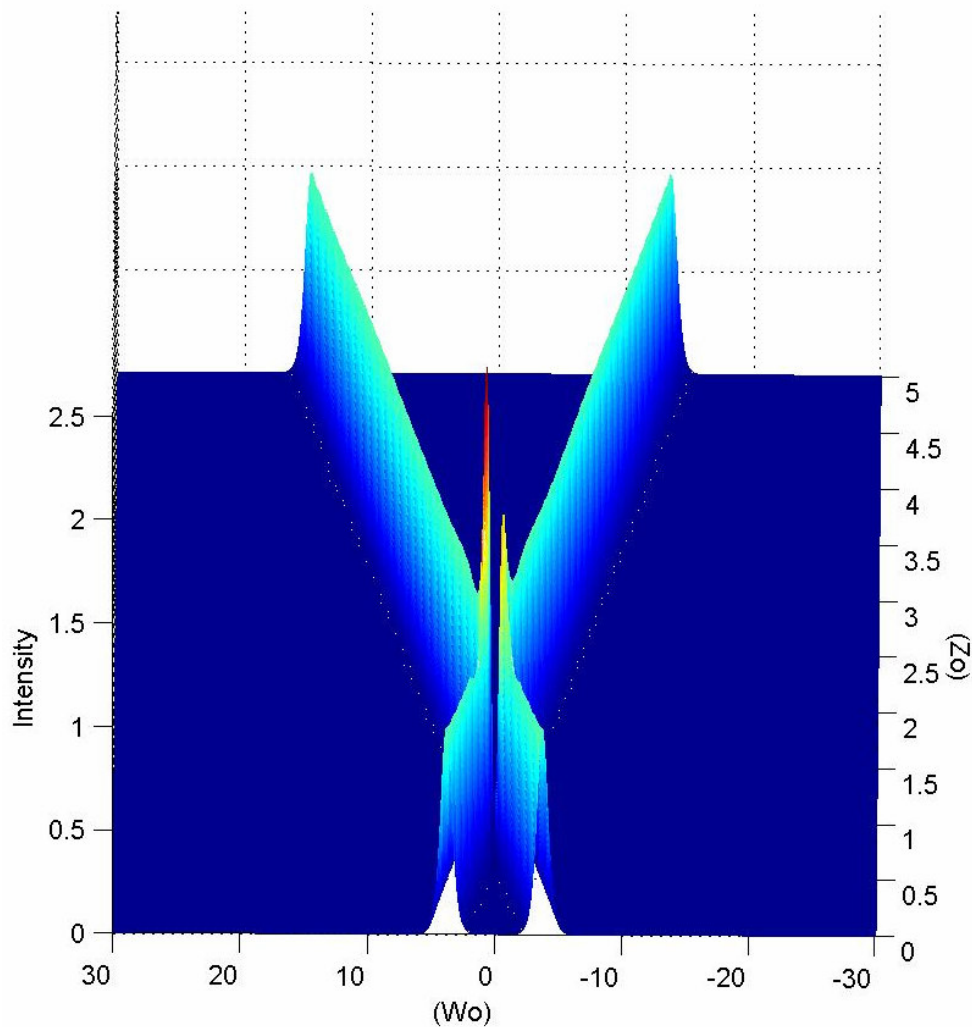


Optical Solitons

ECEN 6016: Nonlinear/crystal optics – Prof. Kelvin Wagner – Fall 2006

Author's numerical simulation of two soliton collision



Sri Rama Prasanna Pavani

pavani@colorado.edu

1. Introduction

The goal of this project is to analyze the properties of optical solitons.

Light diffracts as it propagates in a medium. In linear homogeneous media (air, water), there is no physical phenomenon that restricts diffraction. However, in nonlinear media exhibiting Kerr effect, the diffraction can be controlled by a focusing effect that tries to literally squish the spatial extent of the beam. This rather special effect can be seen typically at very high intensities. According to the optical Kerr effect, the refractive index of nonlinear media increases proportional to the transverse intensity profile of the beam. For instance, if the beam were to have a Gaussian profile, the central part of the beam is more intense than the sides, and hence the media transforms itself into a kind of a GRIN structure, whose refractive index in the center is higher than that of the edges. In other words, the media is transformed to a positive gradient index lens, and hence the focusing effect. If this focusing effect keeps converging a beam, the beam intensity per unit area of the nonlinear medium (Ex: crystal) increases, and at some point, this intensity goes beyond the maximum tolerable intensity level of the crystal, there by physically damaging the crystal. This is often considered as a singularity. However, other mathematical explanations can be found in the literature [1]. On the other hand, when the focusing effect is matched exactly to compensate the diffraction, the beam propagates without any change in the spatial profile. In other words, the beam does not diffract any more. Such, spatially unchanging beams are known as spatially solitons.

As very high peak intensities are required for seeing this magical phenomenon, typically pulsed lasers are used. Pulses disperse as they propagate in fibers. When this dispersion is compensated by self phase modulation (also due to Kerr effect), the temporal shape of the pulse remains a constant. Such pulses are known as temporal solitons.

The forthcoming pages are organized in the following way: While the section 1 reviews the theory of optical solitons, the section 2 illustrates the properties of solitons with

numerical simulations performed by the author. Section 3 has conclusions, Section 4 has acknowledgements, Section 5 lists some important references, and section 6 (Appendix) has MATLAB functions used for numerical simulations.

2. Solitons

This section is essentially a brief summary of chapters 2 and 4 of Prof. Steve Blair's classic thesis on optical solitons [1]

Physical solitary waves were first observed in water waves (J. S. Russell, 1834). After over a century, optical solitary waves were studied in the context of self trapping (Chiao, 1964). Self focusing, which was initially considered problematic, was later recognized as a method for generating spatial solitons. Besides self focusing, other nonlinear mechanisms like Stimulated Raman Scattering (SRS), thermal nonlinearity, and plasma filaments can also lead to soliton solutions. However, this project will concentrate on the Kerr effect based soliton solutions.

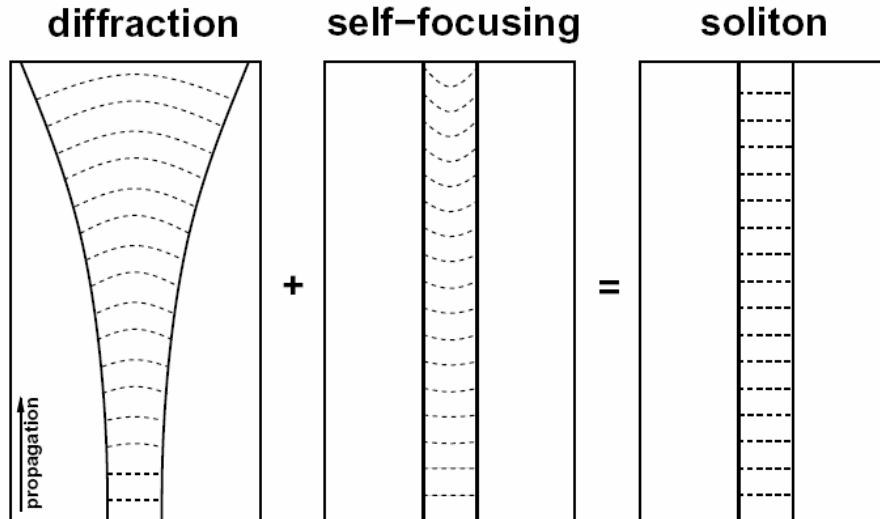
The nonlinear equations that describe a linear scattering problem have bound state eigen values that correspond to soliton solutions. The study of such non linear integrable equations is an active field of research in mathematics. Optical Kerr effect leads to an integrable non linear schrodinger equation both in space and time, which can essentially be used to describe the optical properties of solitons. Optical solitons form when the total refractive index seen by a beam is

$$n = n_0 + n_2 |A|^2$$

Where n_0 is the linear index of the medium, n_2 is the kerr index, and A is the electric field envelope of the incident field. As noted earlier it can be seen that the total refractive index of the medium increases as the amplitude increases.

2.1 1-D spatial solitons

The following figure illustrates the idea behind spatial solitons. The expanding wavefront due to diffraction is exactly compensated by the converging wavefront due to self focusing to produce a soliton with a plane wavefront.



1-D soliton solutions are known to be stable. In other words, the perfect balance between the linear (diffraction) and nonlinear (self focusing) effects prevents small field fluctuations from destroying the soliton. Specifically, if the fluctuation results in a bit of soliton widening, the self-focusing effect gets into the situation to squish the soliton back to its original spatial width. Alternatively, if the fluctuation causes the soliton to get compressed in space, diffraction takes over and makes sure that the soliton is back in its proper form. However, 2-D soliton solutions could potentially become unstable when the diffraction does not balance self focusing, leading to a mathematical singularity. As noted before, the optical consequence of this singularity is (typically) crystal damage.

2.2 1-D soliton solution

As with all other propagation wave solutions, soliton solutions have to satisfy the wave equation. But, now we should consider the nonlinear wave equation. Since we are in the

1D world, we assume that the beam is confined in y axis (physically, consider a slab waveguide). Further, if we assume that the linearly guided and nonlinear soliton envelopes are separable, the general Helmholtz equation reduces to

$$\frac{\partial^2 \bar{A}}{\partial z^2} + \frac{\partial^2 \bar{A}}{\partial x^2} + k_0^2 \bar{A} + 2k_0^2 \frac{n_2}{n_0} |A|^2 \bar{A} = 0$$

Where A is the soliton amplitude, k_0 is the wave number, and n_2 is the nonlinear coefficient. Since a soliton is a stationary solution by definition, we have

$$\bar{A}(x, z) = A(x)e^{i\beta z}$$

Which when substituted into the nonlinear 1D separable wave function, becomes

$$\frac{d^2 A(x)}{dx^2} + \left[k_0^2 - \beta^2 + 2k_0^2 \frac{n_2}{n_0} |A(x)|^2 \right] A(x) = 0$$

where beta represents the total wave number. The transverse envelope is assumed to be of the form

$$A(x) = A_0 \operatorname{sech} \left(\frac{x}{w_0} \right)$$

where

$$A_0 = \frac{1}{\kappa_0 w_0} \sqrt{\frac{n_0}{n_2}}$$

$$\beta^2 = k_0^2, \quad \frac{1}{w_0^2} = k_0^2 \left[1, \frac{n_2 A_0^2}{n_0} \right]$$

Since the wave equation is invariant under unitary transformation, a more general stationary soliton solution can be written as

$$A(x', z') = A_0 \operatorname{sech} \left[\frac{\cos \theta x' - \sin \theta z'}{w_0} \right] e^{i\beta[\cos \theta z' + \sin \theta x']}$$

This is the complete **non-paraxial 1D solution**. Since it is mathematically [1] and numerically difficult to analyze the non-paraxial solution, we make a parabolic approximation that leads to a simple **paraxial 1D solution**

Assume (for simplicity)

$$\bar{A}(x, z) = A(x, z)e^{ik_0 z}.$$

Assume SVEA and make the following approximation

$$\left| \partial^2 A / \partial z^2 \right| = \frac{1}{2k_0} \left| \frac{\partial^3 A}{\partial z^3} + \frac{\partial^3 A}{\partial z \partial x^2} + 2k_0^2 \frac{n_2}{n_0} \frac{\partial |A|^2 A}{\partial z} \right| \ll |2k_0 \partial A / \partial z|$$

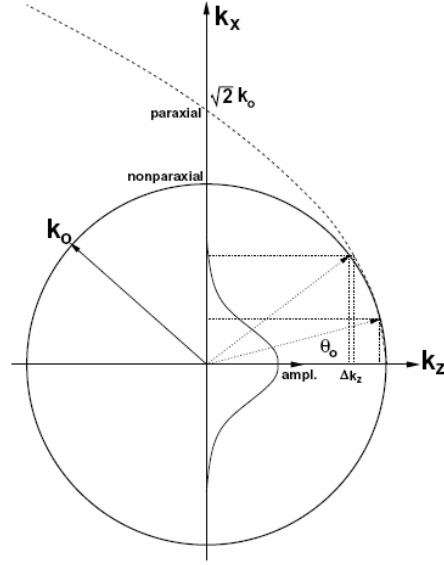
to end up in the following nonlinear Schrödinger equation

$$2ik_0 \frac{\partial A}{\partial z} + \frac{\partial^2 A}{\partial x^2} + 2k_0^2 \frac{n_2}{n_0} |A|^2 A = 0$$

Note that this expression is valid only for propagation along directions very close to z axis. The first two terms of the above expression just represents linear diffraction, while the third term is due to the Kerr nonlinearity.

The following k-space diagram illustrates the paraxial approximation. Diffraction in 1+1 D is represented by slicing the (2+1)D k-surface (sphere) with a plane passing through the origin. As can be seen, the paraxial approximation approximates the k-circle as a parabola, and so, it's accurate only within a small range of angles close to the optical axis.

Mathematically, $k_z = \sqrt{k_0^2 - k_x^2}$ is approximated as $k_z \approx k_0 - k_x^2 / 2k_0$ (retain only the first two terms of binomial expansion)



In the paraxial regime, the general soliton propagation solution can be written as

$$A(x, z) = e^{i\phi^{NL}(x,z)} A(x, 0)$$

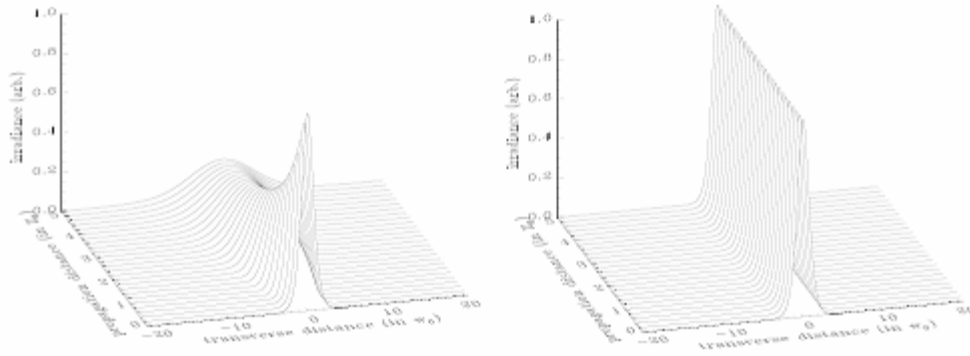
Where $A(x,0)$ is the initial field amplitude and $A(x,z)$ is the field amplitude after propagation through a distance z . The nonlinear phase is the scaled integral of the intensity from 0 to z .

$$\phi^{NL}(x, z) = k_f n_2 \int_0^z |A(x, z')|^2 dz'$$

When z is small, the above equation can be approximated to

$$\phi^{NL}(x, \Delta z) \approx k_f n_2 |A(x, \Delta z/2)|^2 \Delta z$$

The accuracy of numerical beam propagation simulations in linear media does not depend on the z sampling rate. In other words, in linear regime, successively propagating a field through a distance of $10z_0$ ($z_0 = \text{confocal distance}$) in steps of z_0 , will produce the same result as propagating the field directly through $10z_0$. However, in a nonlinear regime, if the above approximation (z is small) is made, z sampling indeed determines the accuracy of propagation. The above paraxial version of the 1D soliton solution forms the basis of the second section of this project.



The above simulation compares the propagation of a beam (diffracting) in a linear media with a spatial soliton. Note that the initial beam profile was same (hyperbolic secant) in both cases. Clearly, the spatial profile of the soliton remains the same as the initial profile even after propagation through $5z_0$!

Such nonlinear simulations involve operations both in space and spectral domains. Propagation is typically done in the fourier domain while the nonlinear effect is added after transforming the field back to the space domain.

By using the stationary ansatz specified before,

$$\frac{d^2 A(x)}{dx^2} + 2k_0 \left[-\beta + k_f n_2 |A(x)|^2 \right] A(x) = 0.$$

Assuming the soliton to be of the form of a hyperbolic secant (defined earlier), the amplitude and phase become

$$A_0 = \frac{1}{k_0 w_0} \sqrt{\frac{n_0}{n_2}}$$

$$\beta = 1/2 \kappa_0 w_0^2 = \kappa_f n_2 A_0^2 / 2$$

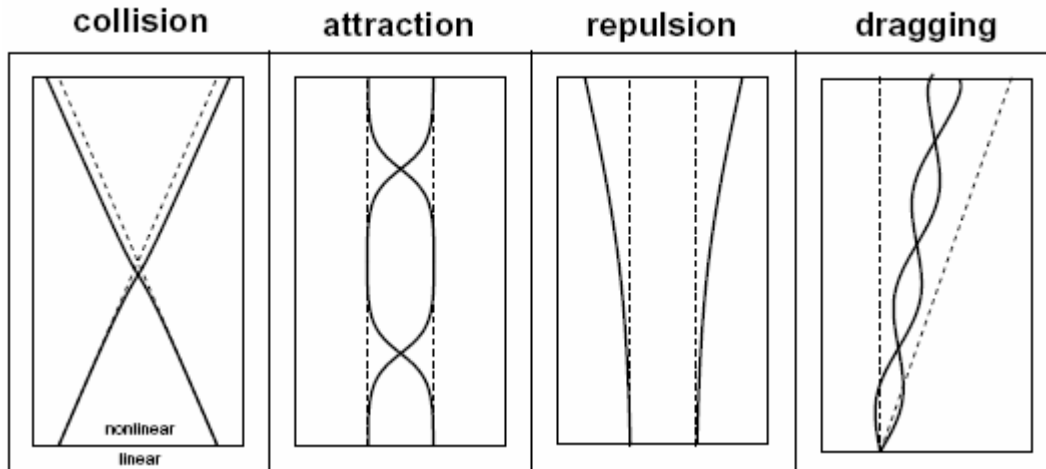
The amplitude remains the same as before while the phase has clearly been changed by the paraxial approximation. Now that we know the amplitude and phase, the full paraxial solution can be expressed as

$$\bar{A}(x, y, z) = \frac{1}{k_0 w_0} \sqrt{\frac{n_0}{n_2}} \Phi(y) \operatorname{sech}\left(\frac{x}{w_0}\right) e^{i[k_0 + 1/2 k_0 w_0^2]z}$$

Let's analyze the above solution. At $z = 0$, we have a real hyperbolic secant. As the soliton propagates ($z > 0$), the amplitude remains the same (amplitude has no z dependence), while there's a linear phase accumulation. As the intensity of the beam is given as square of the absolute value of amplitude, we see that the intensity has no z dependence too! Hence, as advertised, the spatial profile of the soliton is unaffected by propagation.

2.3 Soliton interactions:

The first detailed study on interaction forces in solitons was done by J.P. Gordon in 1983 [3]. Some notable soliton interactions are collision, attraction, repulsion, trapping, and dragging.



Collision interaction between two similarly polarized solitons almost does nothing to the solitons, but for a very small spatial shift, as shown above. As the attractive forces between solitons are balanced both before and after the point of collision, the interaction is symmetric. However, collision interaction between two orthogonally polarized solitons can result in a permanent angle change.

When two similarly polarized solitons with same phase propagate close to each other, they attract. The attraction is periodic in the sense that the two interacting solitons swap spatial positions repeatedly at the same rate as they propagate. Other than this periodic spatial movement, the solitons remain intact. On similar lines, when two similarly polarized solitons with phase difference of $\pi/2$ propagate close to each other, they repel. In contrast to attraction, there is no spatial periodicity in repulsion – The two interacting solitons keep moving away from each other. Attraction and repulsion occur in orthogonally polarized solitons too [1].

Spatial trapping and dragging are asymmetric interactions, where two solitons overlap in the beginning of the nonlinear medium. Since there is no interaction force before overlap, and since the force after overlap is unbalanced, the interacting solitons incur a permanent angle change.

Threshold contrast is a metric to evaluate the potential for a soliton interaction to be useful in applications like logic gates. It is defined as the ratio of the power of the input fundamental signal to the power of the deviated pump that exits the aperture. Pump power, signal power, gate length, aperture size, and interaction length are few parameters that determine threshold contrast. As hinted earlier, an interaction with high threshold contrast is suitable for logic gates.

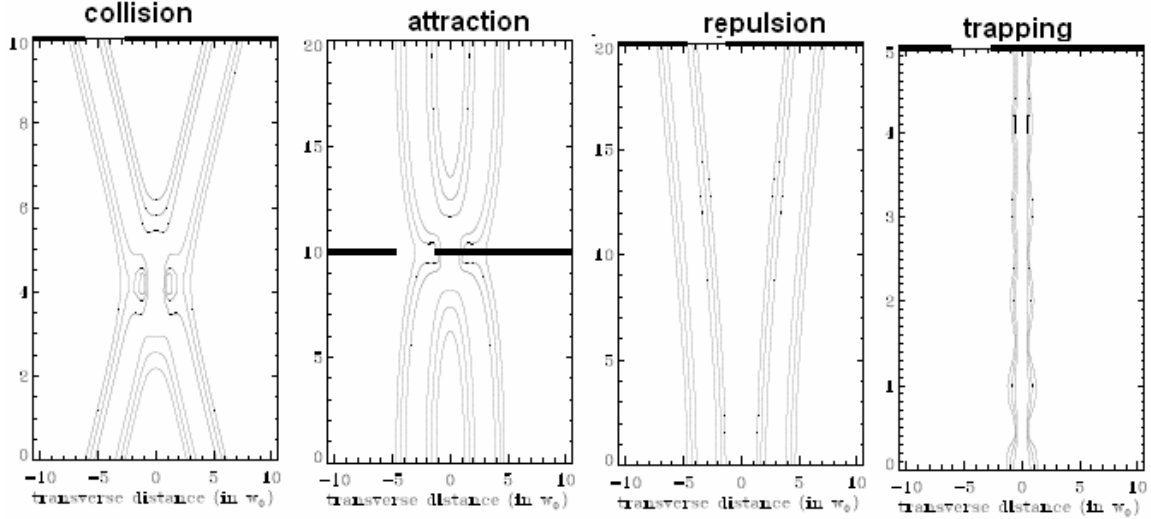
Soliton interactions can be classified as phase sensitive (same polarization) and phase insensitive interactions (orthogonal polarization)

2.4 Phase sensitive interactions

The amount of spectral overlap between two solitons determines the phase sensitivity of an interaction. A very small spectral overlap will almost result in a phase insensitive interaction as the solitons will pass through each other with relatively large velocity.

This would result in a weak interaction. On the other hand, if the spectral overlap is significant, the phase sensitive interaction is strong (useful for high contrast logic gates).

Since the interaction heavily depend on the relative phase of the two solitons, it might be experimentally difficult to control the interaction, and so, these phase sensitive interactions are not widely used for robust logic gates [1] In a collision interaction, the spatial shift decreases with increasing angle of collision. (This is sometimes a problem, because long interaction lengths are required to achieve high contrast by using small collision angles)



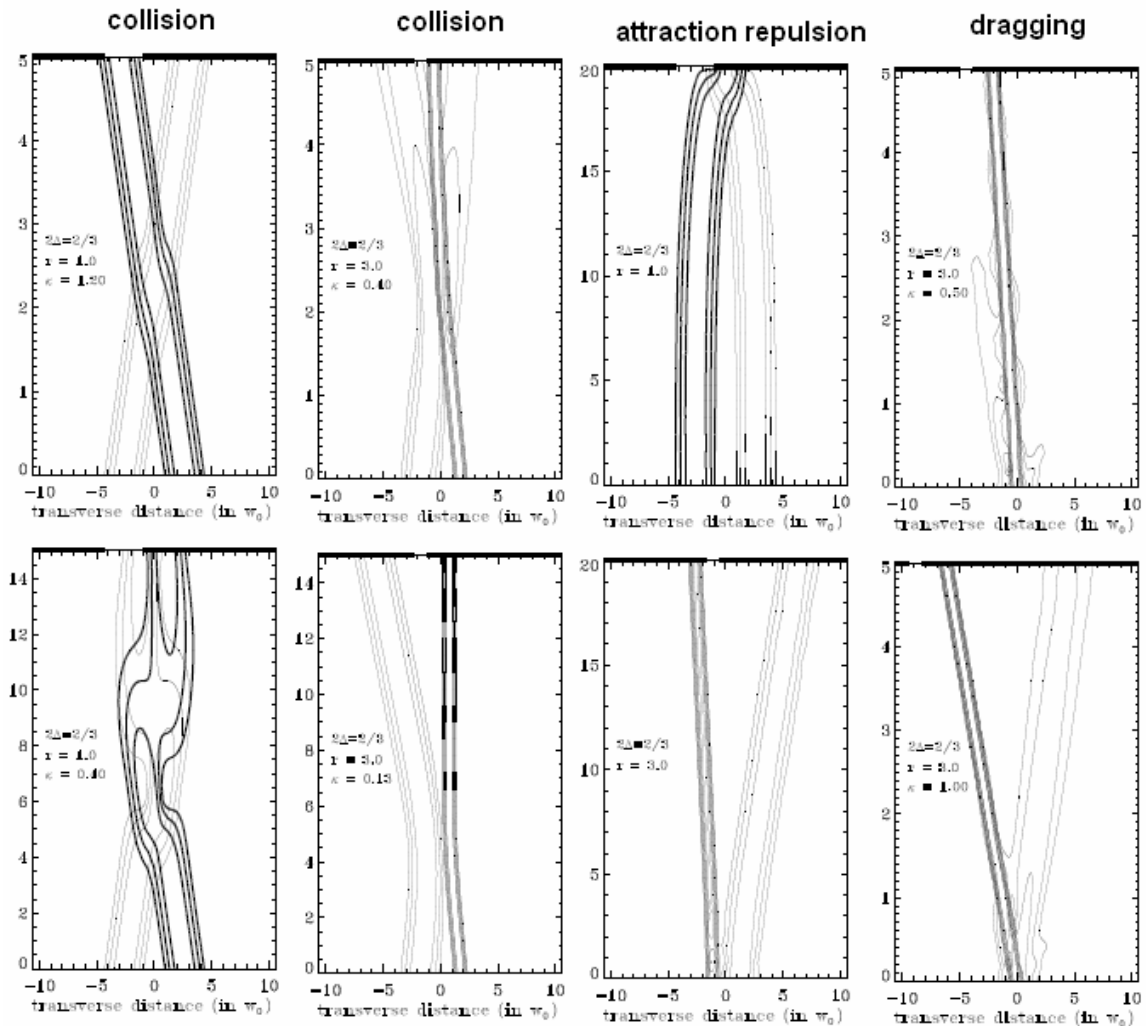
Consider the phase sensitive interactions shown above. The collision interaction ($10Z_0$) gives a threshold contrast of 1.5. While the attraction interaction ($20Z_0$) has a threshold contrast of 4.8, the repulsion interaction ($20Z_0$) gives a contrast of 5.5. Finally, the trapping interaction ($5Z_0$) achieves a contrast of 11. In the collision, repulsion, and trapping interactions, the angular shift due to the interaction can be clearly seen. Note that in each of the above scenarios; had it not been for the interaction, the soliton propagating from right to left would have impinged on the region shown with a small discontinuity.

2.5 Phase insensitive interactions:

In large scale computing systems, phase dependence of an interaction might be annoying. Phase independent interactions can be achieved using orthogonally polarized solitons. For example, in a nonlinear Kerr material, phase-insensitive nonlinear cross-focusing can be used to achieve soliton interactions. In a pseudo-1D soliton interactions, the phase dependence can be completely eliminated. The phase dependence can be reduced in the

case of orthogonal linear polarizations by using waveguide birefringence to mismatch the phase dependent terms in the induced nonlinear material polarizations.

Consider the first phase insensitive collision interaction illustrated below. Here the two solitons have equal amplitudes. The top interaction (5Zo) has a threshold contrast of 1.1 while the bottom interaction (15Zo) has a threshold contrast of 23. In the second phase insensitive collision interaction, the amplitudes of the two solitons are unequal. The top interaction (5Zo) has a threshold contrast of 9.6 and the bottom interaction has a threshold contrast greater than 1000! The attraction interaction (20Zo) between two equal amplitude solitons achieves a contrast of 9.8, while the repulsion interaction (20Zo) between unequal amplitude (3:1) solitons achieves a contrast of 69! The dragging interaction (contrast > 1000) clearly shows an angle shift due to mutual trapping.



3. Numerical Simulations

The numerical simulations of this section were implemented in MATLAB using the split step beam propagation method. Soliton propagation, as described before, involves simultaneous action of linear diffraction and nonlinear self focusing.

Linear diffraction can be thought of as a filtering problem. In other words, the diffracted field is calculated (well, defined) as the convolution of the input field and the impulse response of free space. Since the FFT era, Fourier domain processing has become so fast ($N \log(N)$) that almost all digital filtering operations are performed in the spectral domain, where spatial convolution transforms to spectral multiplication. Hence, the diffraction is implemented in the Fourier domain by just multiplying the Fourier transform of the input field with the free space transfer function. Self-focusing is a nonlinear effect, and so, is generally implemented in the spatial domain.

The following simulations come under the category of (1+1)D beam propagation, where we consider only one transverse dimension (y or x), and the propagation dimension (z). Consider the input field to be $A(x, z = 0)$. The transverse plane at every $z > 0$ represents the propagated field at that particular z .

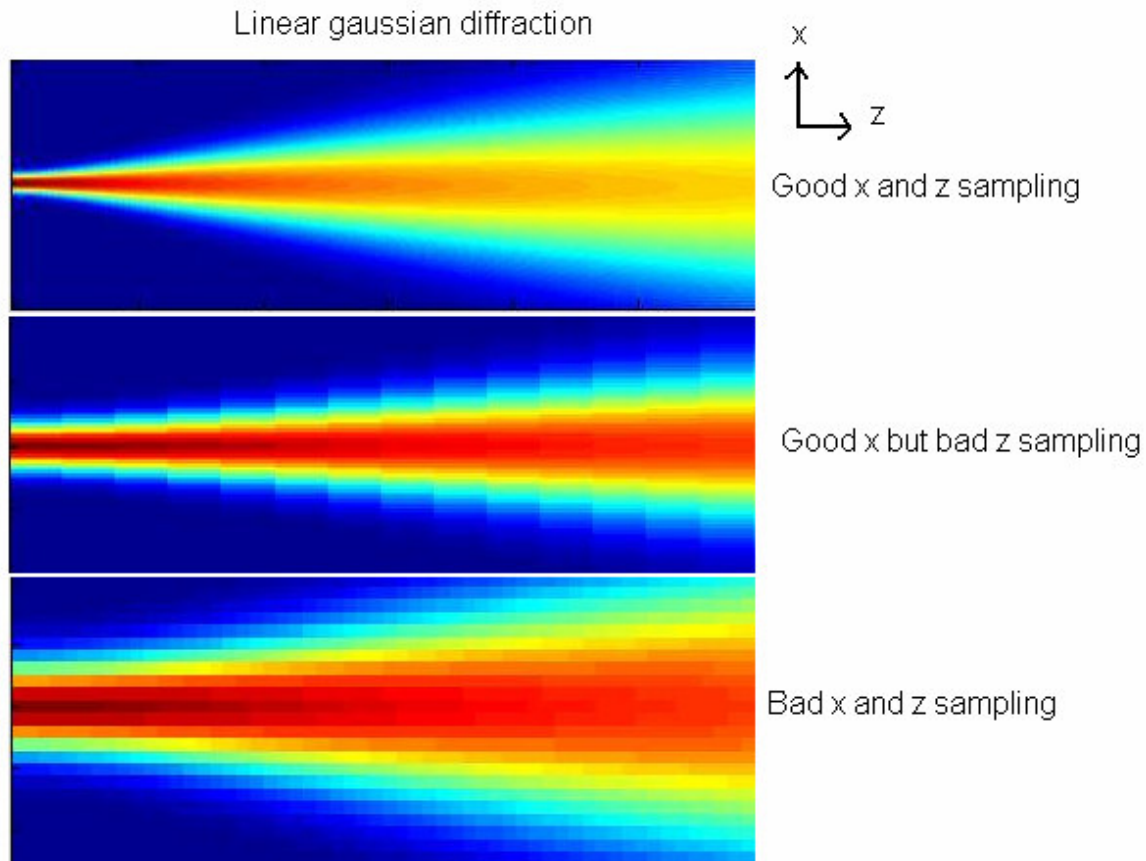
3.1 Sampling:

Digital simulations operate on discrete spatial coordinates, where a continuous function (in x) is represented as a series of quantized samples. In order to avoid aliasing, Nyquist must be obeyed in the transverse dimension. However, this is not necessarily true in the propagation (z) dimension.

Sampling in linear propagation simulations:

Since diffraction can be modeled as a linear system, repeated (' n ' times) filtering of a signal with a filter H is entirely equivalent to applying *one* new filter T to the signal, where the new filter T is just the product of all the repeated filters H in Fourier domain. In other words, $T = H.H.H.....H = H^n$. Hence, in a linear propagation problem low z

sampling will not result in a numerical error. Nevertheless, linear beam propagation simulations used for display generally obey Nyquist (they don't have to). If Nyquist is violated in z , while looking at the entire simulation, there would be very prominent blocking artifacts, which essentially are manifestations of a higher spatial frequencies being misrepresented as lower spatial frequencies.



To summarize, in linear propagation, Nyquist is necessary in the transverse dimension but not in the propagation dimension (z), although obeying Nyquist in z would result in visually appealing simulations.

Sampling in nonlinear diffraction simulations:

In nonlinear propagation simulations involving nonlinear operations in the real space, a very high sampling rate (at least Nyquist) must be maintained in both transverse and the propagation dimensions. High sampling rate in transverse dimension, as before, is to

avoid aliasing, while high sampling in the propagation dimension is necessary to ensure the accuracy of the simulation. A low z -sampling rate will almost certainly result in steep numerical errors. This is because of the following reason:

$$\phi^{NL}(x, z) = k_f n_2 \int_0^z |A(x, z')|^2 dz'$$

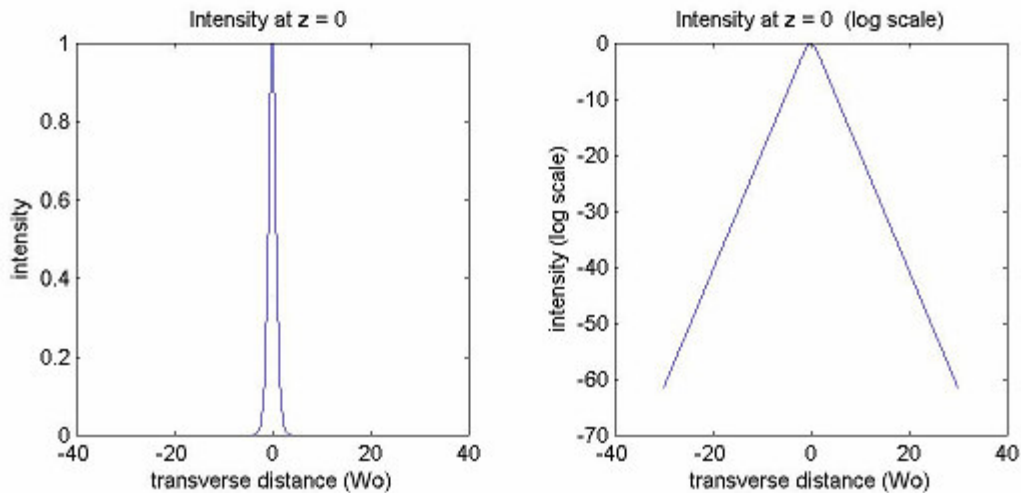
The above function represents the phase to be multiplied in real space in each propagating step. When z is small, this can be approximated to

$$\phi^{NL}(x, \Delta z) \approx k_f n_2 |A(x, \Delta z/2)|^2 \Delta z$$

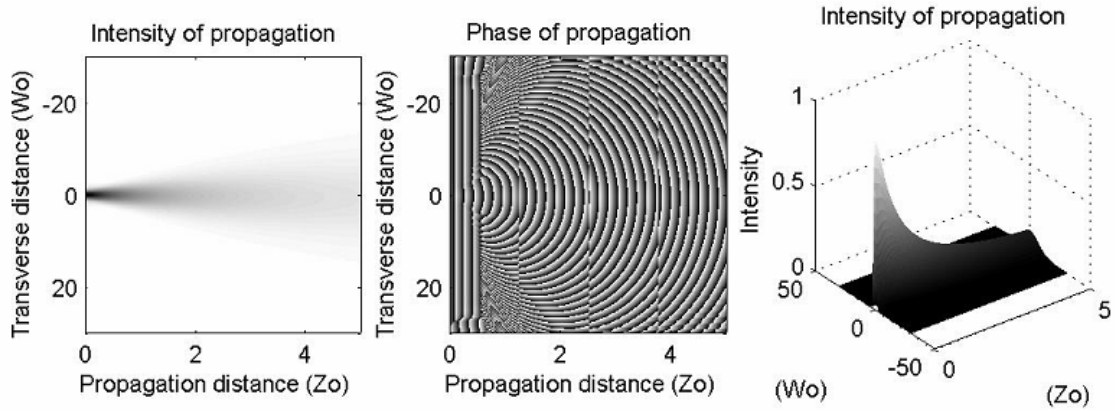
The above phase is relatively much simpler to numerically implement than the earlier expression. But, it's an approximation, and just like any other approximation, it breaks down if it's used in unwarranted regimes. In this case, the valid regime is “small z ”, which corresponds to high sampling rate.

3.2 Spatial solitons

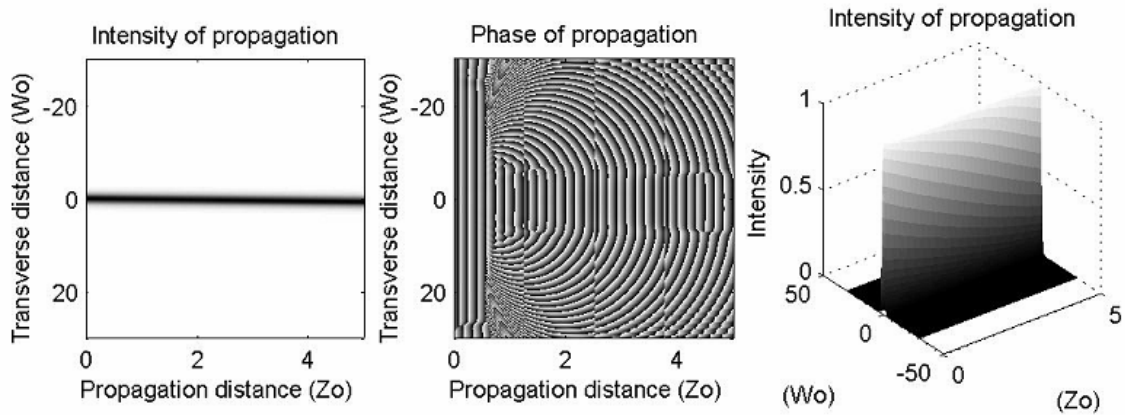
We now simulate the various properties of solitons that we described in section 1. While doing so, we'll also compare soliton propagation with linear diffraction, assuming identical initial fields $A(x, z = 0)$. Hyperbolic secant soliton solutions will be used in all of the following simulations.



When these sech fields propagate in a linear medium, they diffract.

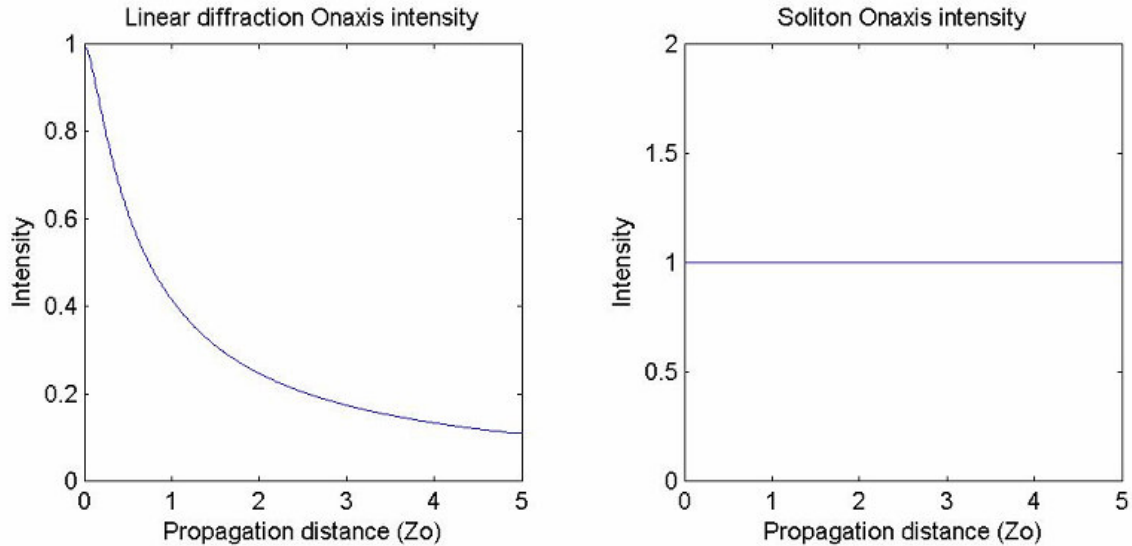


The intensity image clearly shows the energy spreading out as the sech propagates in z . The phase shows expanding spherical wavefronts. The three apparent vertical discontinuities in the phase plot are not real. They are artifacts caused by MATLAB while making the phase image small enough to fit this paper. The 3D intensity plot shows the intensity draining out as it propagates. In this simulation, we propagate until $5Z_0$ using 512 samples both in the transverse and propagation dimensions.



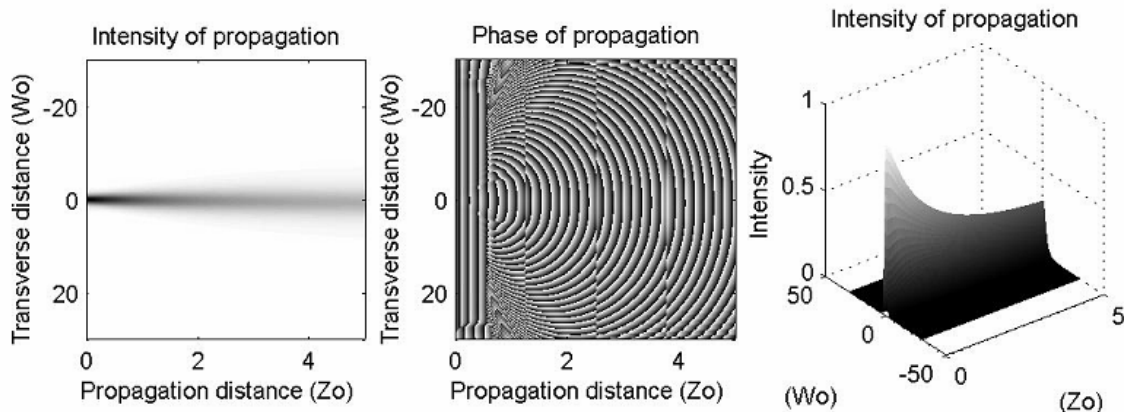
We now consider the paraxial soliton propagation with exactly the same specifications (sampling rate, distances, etc) as before. This was implemented by adding an additional “focusing” step in real space. Specifically, after every diffraction step in fourier space, we come back to the real space and multiply the field with the nonlinear phase defined earlier.

The intensity image shows that there's no spreading out of energy as the sech propagates until $5Z_0$. The number $5Z_0$ was chosen from [1]. The phase image has interesting facts to observe. Any unchanging wave (Ex: Collimated beam) should have a plane wave front, and so should a soliton. It can be clearly seen from the phase image that the central region (where the soliton propagates) has plane wavefronts throughout $5Z_0$. The 3D plot also indicates that the beam loses no energy as it propagates.



Welcome to the world of solitons! Since we now have a fully working soliton numerical algorithm, soliton interactions can be implemented with ease.

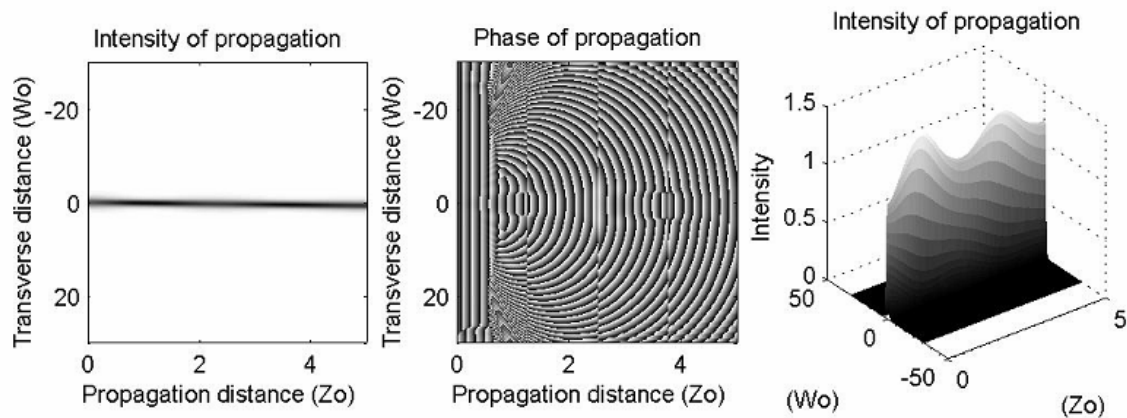
Before jumping into soliton interactions, it might be worth while to analyze the importance of nonlinear phase that exactly compensates diffraction.



If the magnitude of the self focusing effect is lesser than that of diffraction, then the beam will start diffracting as it propagates (although, the diffraction will be at a much smaller rate than what would have been without self focusing) In the above simulation, the self focusing does not exactly compensate diffraction. Compare this with the first simulation, where we did not have self focusing at all. It can be immediately seen that with self focusing, the beam diffracts at a slower rate.

Now, let us consider the other case, where the magnitude of self focusing is larger than that of diffraction. Theoretically, we'd expect the beam to focus down as it propagates. In order to implement this, we slightly increase the magnitude of the nonlinear phase. The results match with theoretical predictions quite amazingly.

Consider the intensity image below. A careful look would reveal that as the beam propagates, the intensity increases and decreases as a continuous function due to “over focusing”.



The phase image is more intuitive. It clearly indicates two “focal points” within the propagation regime. The “focal points” can be identified by the transformation of a converging spherical wavefront into a plane wavefront and then to a diverging spherical wavefront. The 3D intensity image also gives this intuition. In each of the two “focal points”, the intensity is clearly higher.

It's interesting to analyze how diffraction and self focusing try to dominate each other in this simulation. To start with, as self focusing magnitude is higher, the beam starts converging towards a focal point. Beyond the focal point, the beam diverges. Diffraction seems to facilitate this divergence until self focusing starts dominating again.

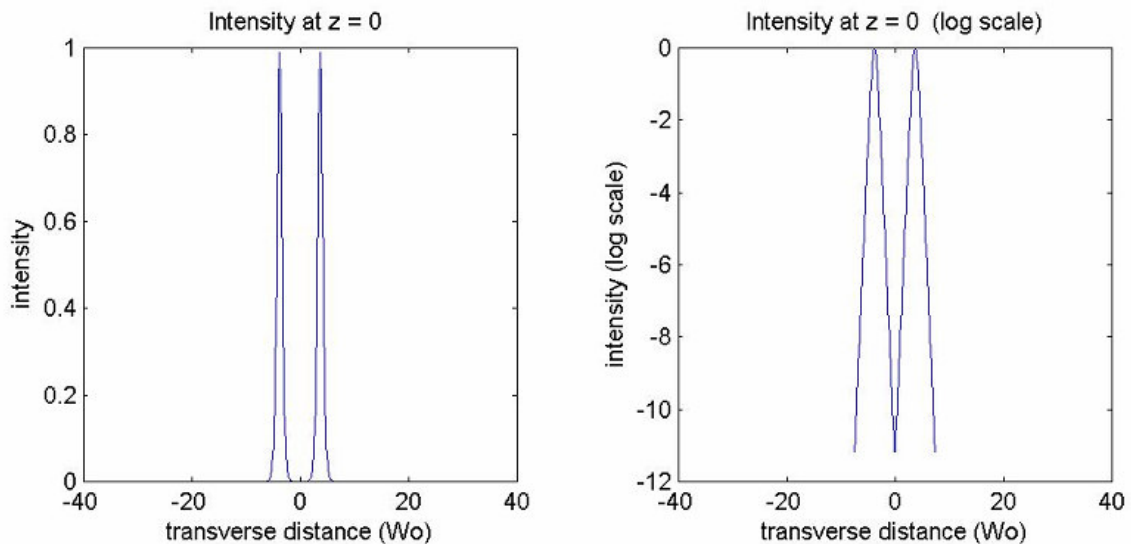
Therefore, for the creation of a soliton, self focusing should exactly (magic?) compensate diffraction.

Soliton interactions:

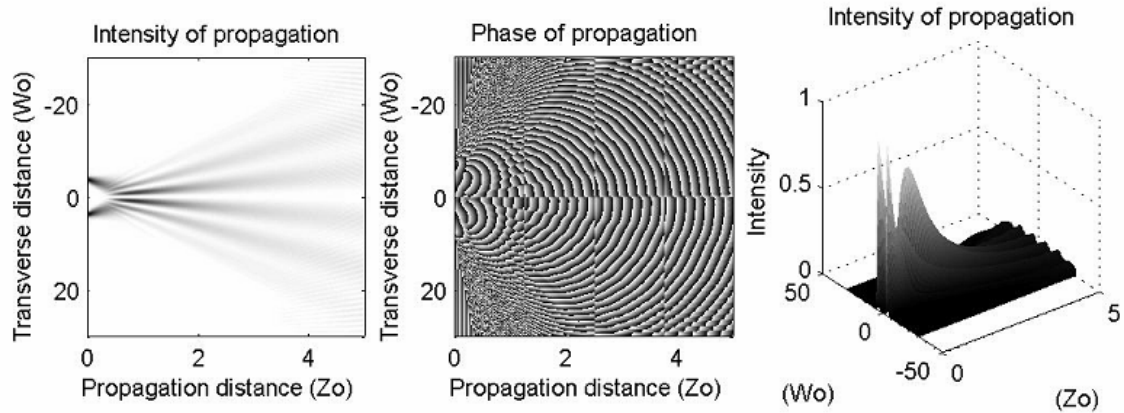
3.3 Soliton Collision:

In this section, we will work with multiple sech fields to analyze soliton interactions. First, we'll let two sech fields to collide both in a linear medium and in the more interesting nonlinear medium (soliton collision).

We implement collision by adding equal but opposite linear phases to two sech fields located close to each other.

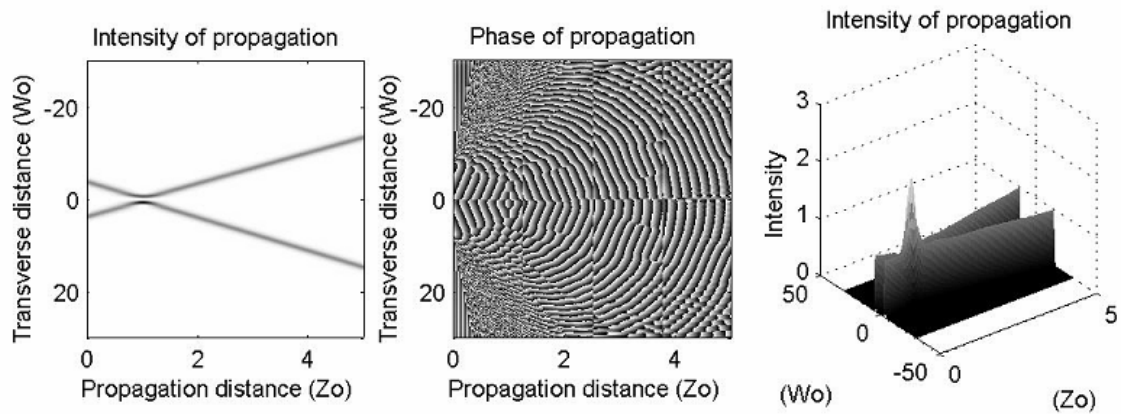


Optically, it's akin to passing two sech fields through two prisms with equal but opposite slopes. An axicon with its center matched to the center of the two sech fields could be one possible lab setup.



The above simulation illustrates the “collision” of two sech beams in a linear medium. Interference fringes can be seen the far field.

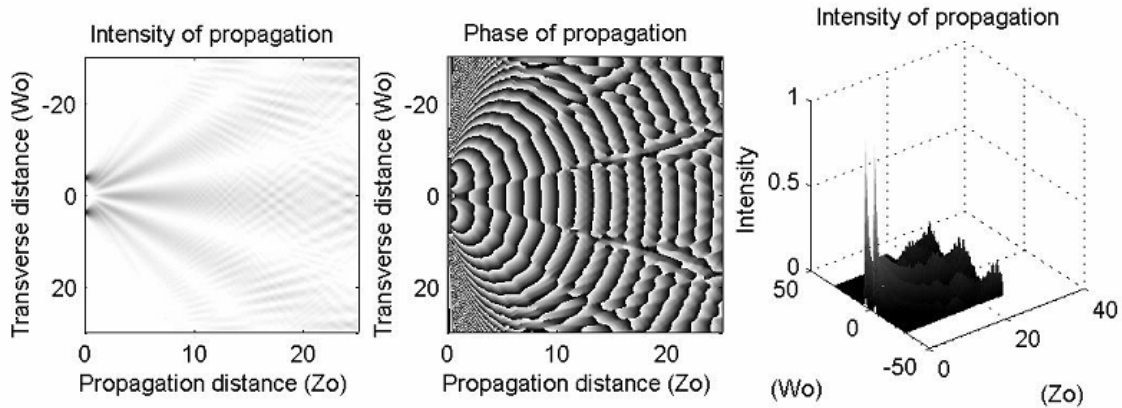
We now implement a two soliton collision. The intensity image clearly shows that the solitons remain unchanged after collision.



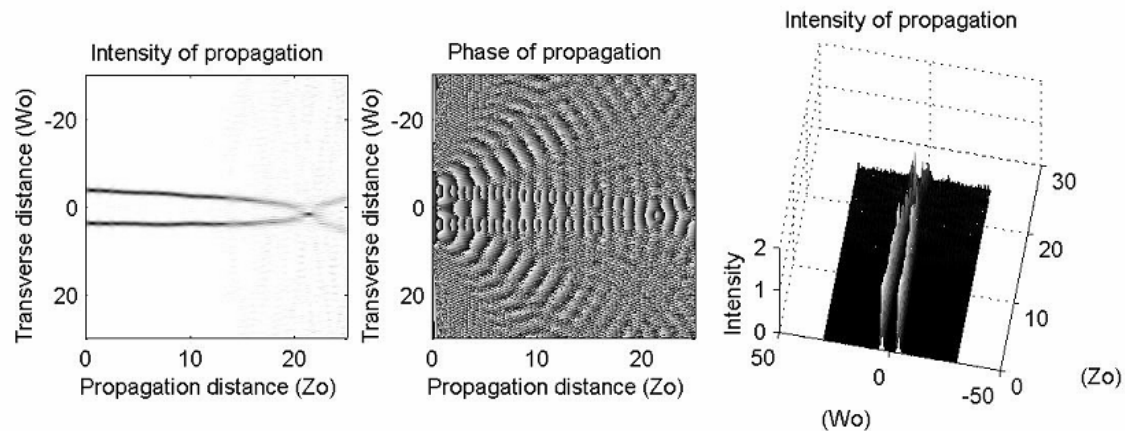
It is interesting to see an (on axis) amplitude null exactly when the two solitons collide. The solitons seem to exactly destructively interfere in that region. Due to the onaxis null, there’s an onaxis phase discontinuity in the phase plot. A careful observation of the phase plot would reveal plane wavefronts in regions of the phase image where the two solitons propagate. There’s a symmetric (transverse) increase in intensity near the overlap region, which can be clearly seen in the 3D intensity plot.

3.4 Soliton attraction:

To implement soliton repulsion, we come in which two sech fields as before, but with no linear phase. In other words, the sech beams are propagating parallel to each other. The tails of the two sech beams overlap a “bit” in linear scale and a “bit more” in log scale.



In the linear simulation, note that onaxis far field is bright. (constructive interference)

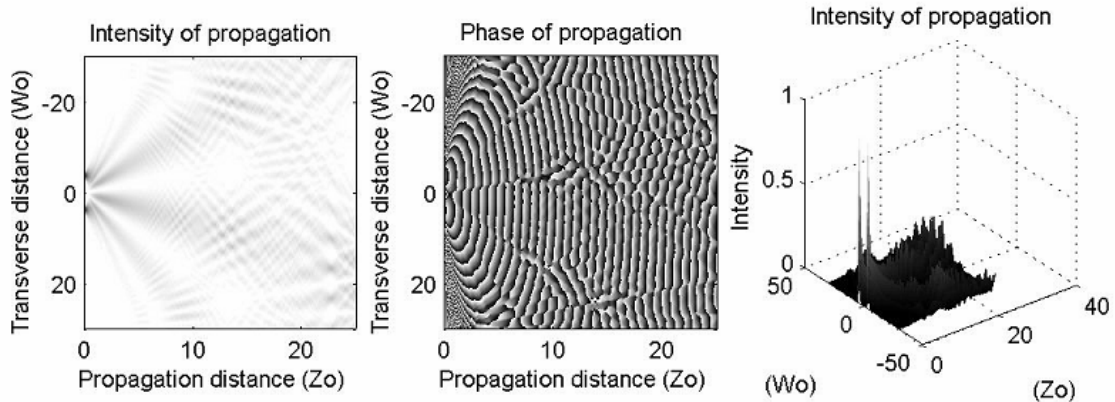


The linear and nonlinear results are shown above. For observing attraction, the author had to propagate the beam through at least $25Z_0$. This probably could be done better if the two sech fields were located even closer. The problem with going through $25Z_0$ is that the z samples become enormous, and in order to make the algorithm execute in a reasonable amount of time, the z sampling frequency was reduced (bad). Since nonlinear propagation numerical errors increase drastically at low sampling frequencies, the above simulation isn't all that accurate. Specifically, the energy of the soliton seems to be decreasing as it propagates (although the locality of the field is conserved). Nevertheless,

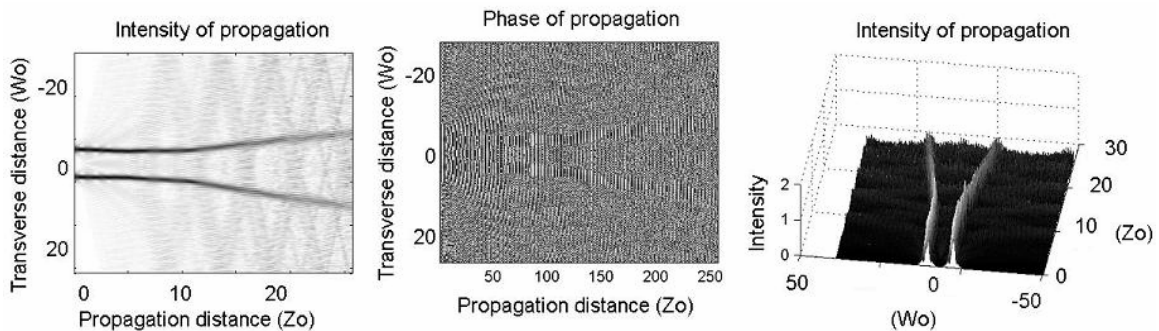
the point here is to prove that solitons do attract, and the attraction can be clearly seen at about $20Z_0$ in all three images shown above.

3.5 Soliton repulsion:

Soliton repulsion is implemented by making one of the two sech fields $\pi/2$ out of phase with respect to the other. The results are shown below.



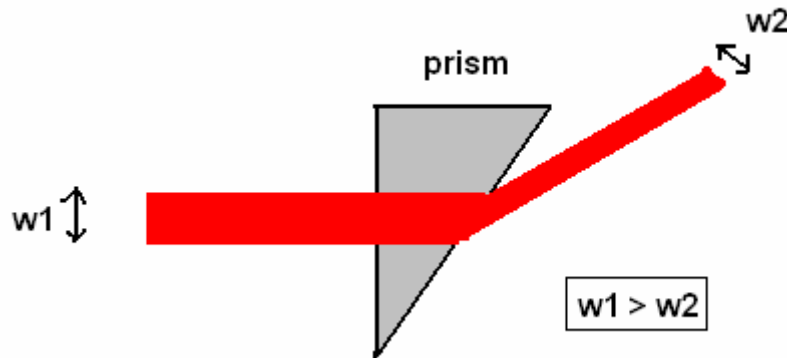
In the linear simulation, note that because of the $\pi/2$ out of phase, on axis far field is not all that bright as before. This is not destructive interference (π out of phase). On axis is in between constructive and destructive interference regimes.



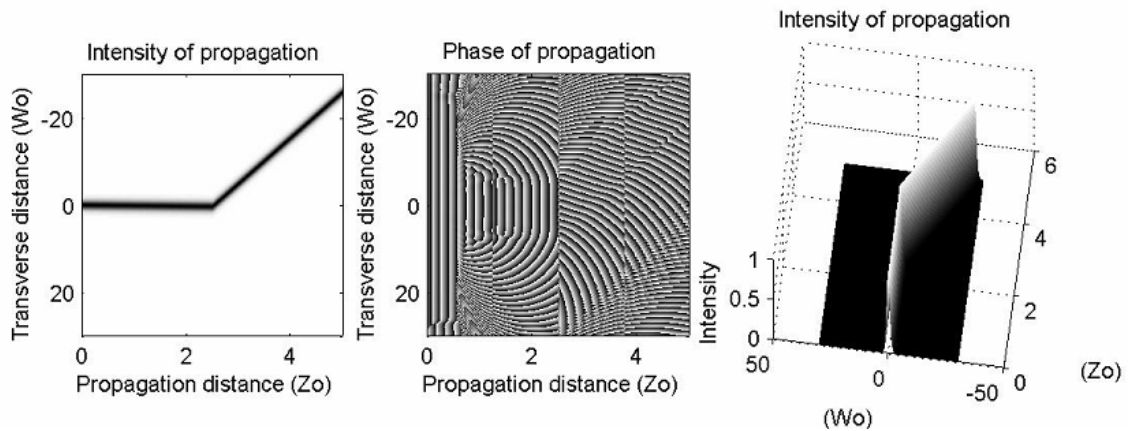
Soliton repulsion results are shown above. Clearly, the two solitons start repelling each other at about $10Z_0$. As explained earlier, the numerical errors are due to lack of adequate sampling in the propagation (z) dimension [computational limitations, as we are propagation until $25Z_0$]

3.6 Soliton propagation through a thin prism:

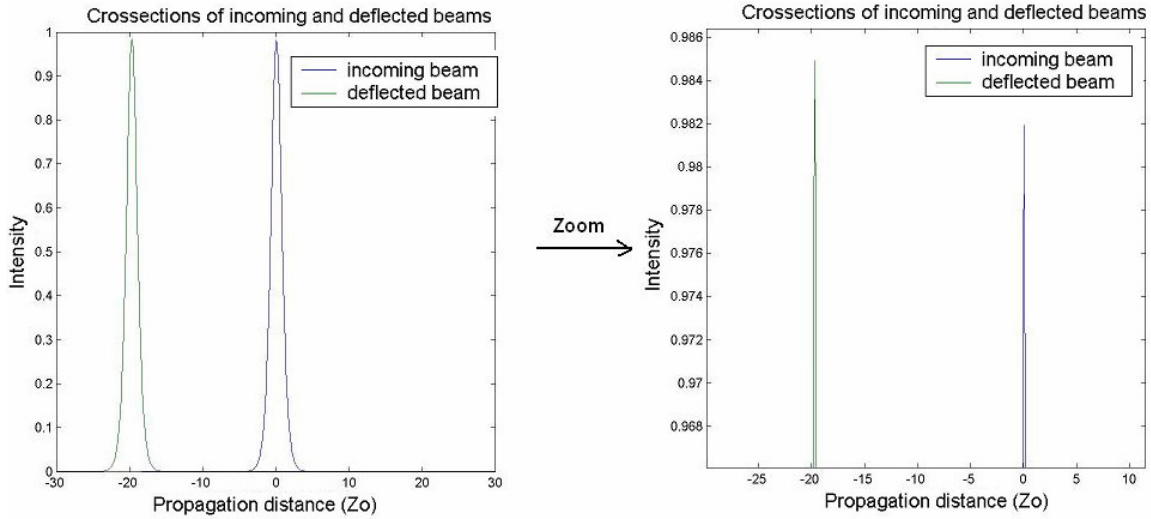
We now simulate the propagation of a soliton through a thin prism. When a beam passes through a prism, it gets deflected. The width of the incoming beam and the deflected beam are not same anymore.



Since the spatial extent of the deflected beam decreases, conservation of energy seems to demand that the peak intensity of the deflected beam should be greater than that of the incoming beam. The goal of this section is to see if a numerical simulation can verify this.



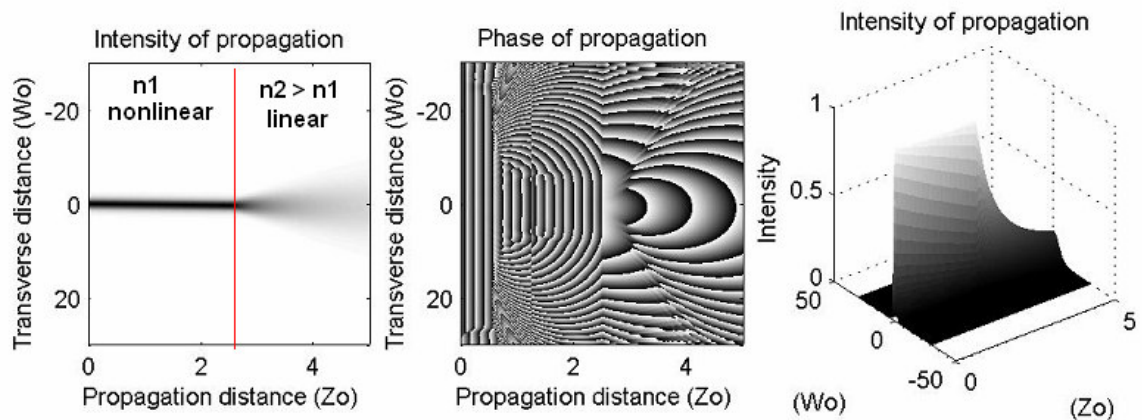
The above simulation was implemented by introducing an inverted thin prism half way through the propagation. From the intensity image, it can be clearly seen that the soliton is deflected. Also, a careful observation would reveal the reduction in the width of the deflected beam. In order to verify the increase in the peak intensity, we analyze a transverse cross-section of incoming and deflected beams. The results are shown below.



As predicted the peak intensity of the deflected beam is higher than that of the incoming beam.

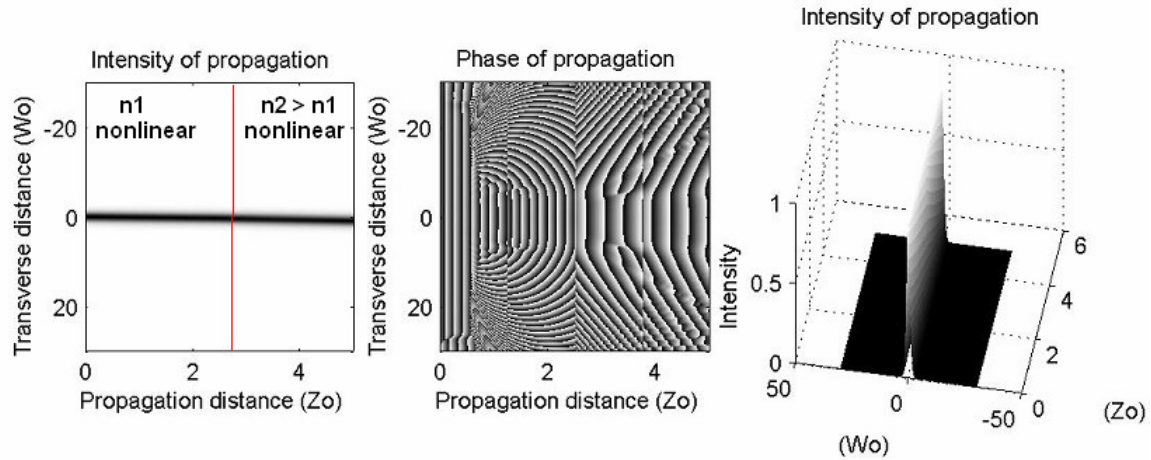
3.7 Soliton transmission through boundaries of two media:

The following simulation simulates the propagation of a soliton from a nonlinear medium into a linear medium of higher refractive index.



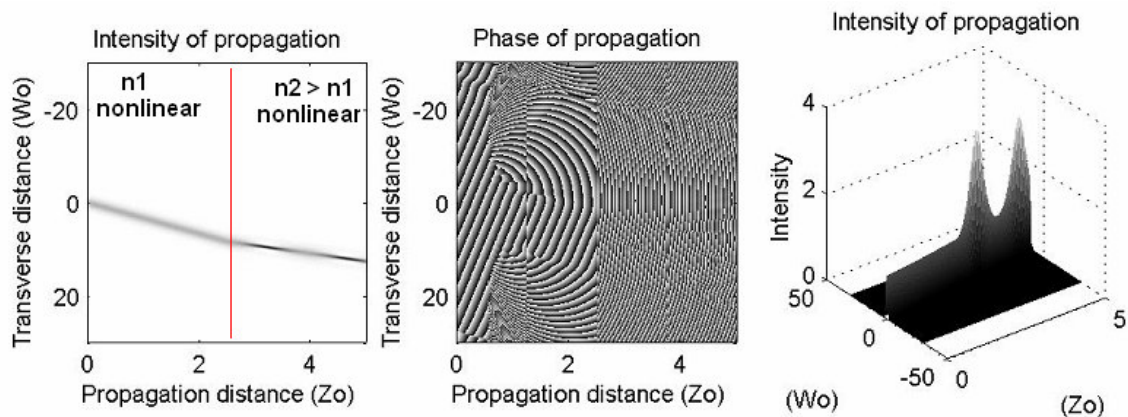
Since the linear media has no self-focussing, the soliton diffracts immediately after it crosses the boundary.

We now consider the propagation of a soliton from a nonlinear medium to another nonlinear medium with a higher refractive index. In doing so, we assume that the self focusing effect in both the media compensates diffraction exactly.

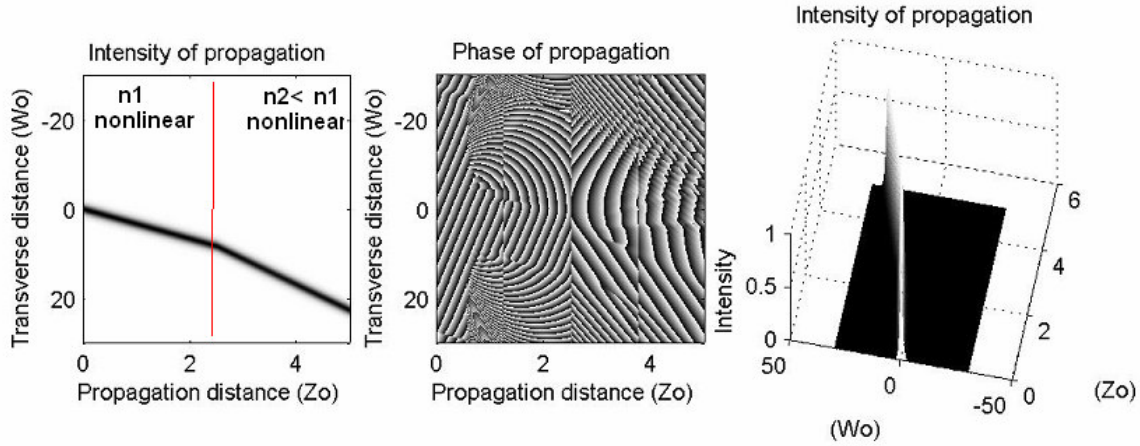


The phase plot is heavily aliased. In a higher refractive index media, the wavefronts should be closer. They are indeed closer in the above phase image. Aliasing is making the high frequencies look like low frequencies.

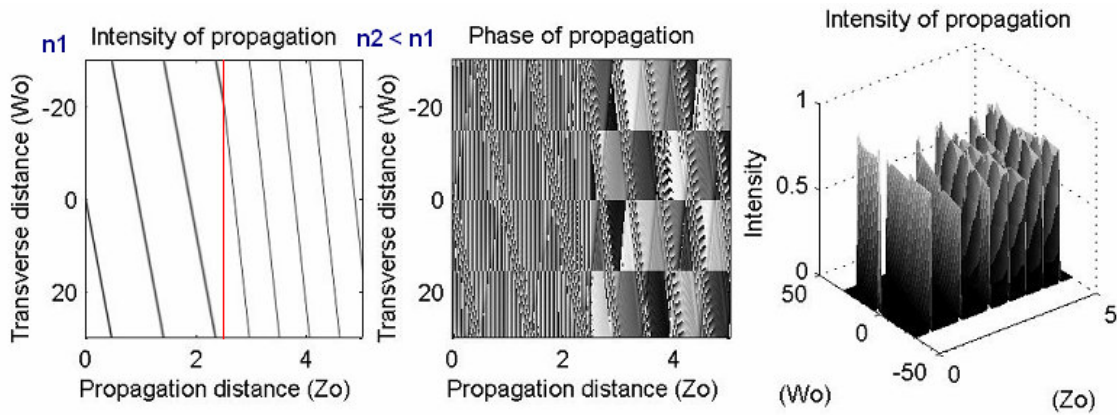
In the above simulation, we assumed normal incidence. When the soliton comes in at an angle, the width of the soliton after the boundary is different from the width before the boundary. Specifically, if the soliton is moving into a higher index medium from a lower index medium, the width increases. Similarly, if the soliton moves into a lower index medium from a higher index medium its width decreases. Needless to say, width is conserved in normal incidence.



In the above simulation, there's too much of self focusing after the soliton enters the new media. As the refractive index of the new media is greater than the old media, the soliton bends towards the normal.



In the above simulation, the soliton passes from a higher index medium to a lower index medium, and so, it deflects away from the normal. A careful observation would reveal that the width of the soliton has reduced after crossing the boundary.



In the above final simulation, the soliton comes in at a very high angle to enter a lower index medium. Because of the finite limits, everytime the soliton crosses the bottom boundary, it appears to come in from the top. Although it appears bit funny, it is numerically correct. The motivation for coming in at a very high angle was to show the considerable width reduction.

4. Conclusion

We first theoretically reviewed the basic principles of optical solitons and their interactions. Later in the second section, we analyzed the properties of solitons rigorously using numerical nonlinear split step beam propagation technique. Soliton propagation was compared to linear diffraction. Soliton interactions were simulated. Next, we moved on to the propagation of soliton through a prism and verified that the peak intensity of the deflected beam is higher than that of the incident beam. Finally, we simulated the behavior of solitons when they cross boundaries of linear/nonlinear media with higher/lower refractive index.

5. Acknowledgements



<http://moisl.colorado.edu>



<http://cdm-optics.com>

6. References

- [1] Steve Blair, “Optical soliton based logic gates”, PhD Thesis, University of Colorado at Boulder, 1998. Download: <http://www.ece.utah.edu/~blair/P/dissert.pdf>
- [2] Balakishore Yellampalle, “Optical soliton controlled inverters in quadratic media and inhomogeneous waveguides”, PhD Thesis, University of Colorado at Boulder, 2004
- [3] J. P. Gordon, “Interaction forces among solitons in optical fibers”, optics letters, vol. 8, pp 596-598, November 1983
- [4] Mollenauer, “Solitons in optical fibers”, Elsevier, 2006
- [5] Prof. Kelvin Wagner – Nonlinear/Crystal optics class notes – Fall 2006
- [6] Prof. Kelvin Wagner – Fourier Optics and Holography class notes – Fall 2005

7. Appendix MATLAB code used for this project

7.1 Soliton.m

```
% action = 0 implies one soliton
% action = 1 implies collision
% action = 2 implies attraction
% action = 3 implies repulsion

function [o] = soliton(isSoliton, action)

if (nargin == 0)
    cc
    isSoliton = 1;
    action = 2;
end

% 1d imaging in beam prop
lam = .632e-6;

% size
N = 256*2;

%object
switch action
    case (0)
        npi = 10;
        o = sech(linspace(-npi*pi,npi*pi,N));
    case (1)
        p = 1e1;
        npi = 2;
        o = sech(linspace(-npi*pi,npi*pi,N/8));
        o = [zeros(1, 3*N/8) o.* exp(i*linspace(0,1,N/8) * p) o .* exp(-
i*linspace(0,1,N/8) * p) zeros(1, 3*N/8)];

%         o = [o .* exp(i*linspace(0,1,N/2) * p) o .* exp(-
i*linspace(0,1,N/2) * p)];
```

```

    case (2)
        2
    npi = 2;
    o = sech(linspace(-npi*pi,npi*pi,N/8));
    o = [zeros(1, 3*N/8) o o zeros(1, 3*N/8)];

        case (3)
            3
    npi = 2;
    o = sech(linspace(-npi*pi,npi*pi,N/8));
    o = [zeros(1, 3*N/8) o o*i zeros(1, 3*N/8)];
end

lt = linspace(-30,30,N);
figure;
subplot(1,2,1); plot(lt,abs(o).^2); title('Intensity at z = 0 ');
xlabel('transverse distance (Wo)'); ylabel('intensity');axis square;
subplot(1,2,2); plot(lt,log(abs(o).^2)); title('Intensity at z = 0
(log scale)'); xlabel('transverse distance (Wo)'); ylabel('intensity
(log scale)');axis square;

% propagation transfer function.
% d = .002;
switch (action)
    case (0)
        d = .002;
    case (1)
        d = .002;
    case(2)
        d = 1.1e-2
    case(3)
        d = 1.1e-2
end

ko = 2*pi/lam;
ky = linspace(-.03,.03,N)/lam;

```

```

H = exp(i* (2*pi/lam) * sqrt(1 - (lam*ky).^2) * d);
% sup(abs(o), angle(o), abs(H), angle(H));

% propagate
steps = 256*2;
lz = linspace(0,5,steps);

I = zeros(steps,N);
I(1,:) = o;
for ii = 2:steps
    I(ii,:) = ift(ft(I(ii-1,:)) .* H);

    if (isSoliton == 1)

        % comment the following line for ordinary (non-soliton)
        diffraction.
        switch(action)
            case (0)
                I(ii,:) = I(ii,:) .* exp(i * abs(I(ii,:)).^2 * .0027e1);
            case (1)

                I(ii,:) = I(ii,:) .* exp(i * abs(I(ii,:)).^2 * .007e1);
            case (2)
                % just ok
                I(ii,:) = I(ii,:) .* exp(i * abs(I(ii,:)).^2 * 7.1e-1);

            case (3)
                % just ok
                I(ii,:) = I(ii,:) .* exp(i * abs(I(ii,:)).^2 * .004e1);
        end
    end
end

% figure;
% subplot(2,2,1);plot(abs(o));
% subplot(2,2,2);imagesc(iminv(abs(I'))); cmg;
% subplot(2,2,3);imagesc((angle(I'))); cmg;
% subplot(2,2,4);mesh((abs(I')));

```

```

figure;
subplot(1,3,1);imagesc(lz,lt,iminv(abs(I').^2)); axis square;cmg;
title('Intensity of propagation '); ylabel('Transverse distance (Wo)');
xlabel('Propagation distance (Zo)');
subplot(1,3,2);imagesc(lz,lt,(angle(I'))); axis square;cmg;
title('Phase of propagation '); ylabel('Transverse distance (Wo)');
xlabel('Propagation distance (Zo)');
subplot(1,3,3);mesh(lz,lt,(abs(I').^2));axis square;title('Intensity of
propagation '); ylabel('(Wo)'); xlabel('(Zo)'); zlabel('Intensity');

figure;
plot(lz, abs(I(:,N/2)).^2); title('Linear diffraction Onaxis
intensity'); xlabel('Propagation distance (Zo)'); ylabel ('Intensity');
axis square;

```

7.2 Soliton through a prism:

```

lam = .632e-6;

% size
N = 256*2;

npi = 10;
p = 000;
o = sech(linspace(-npi*pi,npi*pi,N)) .* exp(i*linspace(0,1,N) * p);

% propagation transfer function.
% d = .002;

d = .002;

ko = 2*pi/lam;
ky = linspace(-.03,.03,N)/lam;
H = exp(i* (2*pi/lam) * sqrt(1 - (lam*ky).^2) * d);
% sup(abs(o), angle(o), abs(H), angle(H));

```

```

% propagate
steps = 256;

I = zeros(steps,N);
I(1,:) = 0;
for ii = 2:steps
    I(ii,:) = ift(ft(I(ii-1,:)) .* H);

    % comment the following line for ordinary (non-soliton)
    diffraction.
    I(ii,:) = I(ii,:) .* exp(i * abs(I(ii,:)).^2 * .0027e1);

end

    I(ii,:) = I(ii,:) .* exp(-i * linspace(1,2,N)* 2.5e2);

for ii = steps+1:2*steps
    I(ii,:) = ift(ft(I(ii-1,:)) .* H);

    % comment the following line for ordinary (non-soliton)
    diffraction.
    I(ii,:) = I(ii,:) .* exp(i * abs(I(ii,:)).^2 * .0027e1);

end

lz = linspace(0,5,512);
lt = linspace(-30,30,512);
figure;
subplot(1,3,1);imagesc(lz,lt,iminv(abs(I').^2)); axis square;cmg;
title('Intensity of propagation '); ylabel('Transverse distance (Wo)');
xlabel('Propagation distance (Zo)');
subplot(1,3,2);imagesc(lz,lt,(angle(I'))); axis square;cmg;
title('Phase of propagation '); ylabel('Transverse distance (Wo)');
xlabel('Propagation distance (Zo)');
subplot(1,3,3);mesh(lz,lt,(abs(I').^2));axis square;title('Intensity of
propagation '); ylabel('(Wo)'); xlabel('(Zo)'); zlabel('Intensity');

```

7.3 Soliton through a boundary

```
function [] = soliton_boundary()
lam = .632e-6;

% size
N = 256*2;

    npi = 10;
    p = 1.5e3;
    o = sech(linspace(-npi*pi,npi*pi,N)) .* exp(i*linspace(0,1,N) * p);

% propagation transfer function.
% d = .002;

d = .002;

ko = 2*pi/lam;
ky = linspace(-.03,.03,N)/lam;
H = exp(i* (2*pi/lam) * sqrt(1 - (lam*ky).^2) * d);
% sup(abs(o), angle(o), abs(H), angle(H));

% propagate
steps = 256;

I = zeros(steps,N);
I(1,:) = o;
for ii = 2:steps
    I(ii,:) = ift(ft(I(ii-1,:)) .* H);

    % comment the following line for ordinary (non-soliton)
    diffraction.
    I(ii,:) = I(ii,:) .* exp(i * abs(I(ii,:)).^2 * .0027e1);

end
```

```

n = 1.2; d=.002
H = exp(i* (2*pi*n/lam) * sqrt(1 - (lam*ky * n).^2) * d);

for ii = steps+1:2*steps
    I(ii,:) = ift(ft(I(ii-1,:)) .* H);

    % comment the following line for ordinary (non-soliton)
    diffraction.
    % n = 1.2
    I(ii,:) = I(ii,:) .* exp(i * abs(I(ii,:)).^2 * .0045e1);
    % I(ii,:) = I(ii,:) .* exp(i * abs(I(ii,:)).^2 * .001e1);

end

lz = linspace(0,5,512);
lt = linspace(-30,30,512);
figure;
subplot(1,3,1);imagesc(lz,lt,iminv(abs(I').^2)); axis square;cmg;
title('Intensity of propagation '); ylabel('Transverse distance (Wo)');
xlabel('Propagation distance (Zo)');
subplot(1,3,2);imagesc(lz,lt,(angle(I'))); axis square;cmg;
title('Phase of propagation '); ylabel('Transverse distance (Wo)');
xlabel('Propagation distance (Zo)');
subplot(1,3,3);mesh(lz,lt,(abs(I').^2));axis square;title('Intensity of
propagation '); ylabel('(Wo)'); xlabel('(Zo)'); zlabel('Intensity');

```